# A Synthetic Nervous System Model of the Insect Optomotor Response

Anna Sedlackova $^1$ , Nicholas S. Szczecinski $^{1[0000-0002-6453-6475]}$ , and Roger D. Ouinn $^{1[0000-0002-8504-7160]}$ 

<sup>1</sup> Case Western Reserve University, Cleveland, OH 44106, USA nss36@case.edu

**Abstract.** We seek to increase the sophistication of our insect-like hexapod robot MantisBot's visual system. We assembled and tested a benchtop robotic testbed with which to test our dynamical neural model of the insect visual system. Here we specifically model wide-field vision and the optomotor response. The system is composed of a Raspberry Pi with a camera outfitted with a 360-degree lens. The camera sits on a motorized turntable, which represents the "robot". Above the turntable sits another motorized system that rotates a drum with printed patterns around the camera, which represents the visual "background". The camera downsamples the visual scene and sends it to a synthetic nervous system (SNS) model of the insect optic lobe. The optic lobe is columnar. Each column detects changes in receptor intensity (retina), inhibits adjacent columns to increase dynamic range (lamina), compares time-delayed activities of adjacent columns to detect motion (medulla), then pools the motion of each column in a directionallyspecific connectivity to compute the direction and speed of the wide-field scene (lobula plate). Our robotic model successfully encodes lateral wide-field visual speed into the activity of a pair of opposing Lobula Plate Tangential Cells (LPTCs). Furthermore, the optomotor response can be recreated by using the LPTCs to stimulate the neck motor neurons (MNs), producing a real-time, closed-loop dynamical model of the optomotor response.

Keywords: Synthetic Nervous System, Optomotor Response, Insect, Vision.

## 1 Introduction

Despite their miniature brains of less than a million neurons, insects are able to solve complex vision tasks - locating prey, avoiding obstacles, tracking prey or mates - all with the use of environmental cues [1]. Insects can still outperform man-made robots and systems in visual tasks despite their limited metabolic and computational power [2]. The basis of this performance is the optic lobe of the insect brain, which uses a parallelized system of functionally-distinct layers to process visual input. Insects' ability to compute optic flow, also called "wide-field vision," has been thoroughly studied [3], but gaps in the knowledge remain. To test how well the current understanding of these networks can explain their function [4], we built an anatomically-constrained

model of the optic lobe using our "synthetic nervous system" (SNS) approach, and use it as the basis of a robotic model of the insect optomotor response.

What is known about the structure of the optic lobe? There are three separate neuropils contained within the optic lobe: the lamina, medulla, and lobula complex, which itself consists of the lobula and the lobula plate (for a review see [3]). Each of the neuropils contains organized columnar units corresponding to the ommatidial (i.e. lens) array in the retina and operates on neighboring columns in each successive layer. The lamina is stimulated by the retina and inhibits its neighboring columns to increase the contrast and dynamic range of incoming images. The medulla appears to correlate the activity of adjacent columns with a time delay in order to detect motion across the retina via "elementary motion detectors" (EMDs), the precise structure of which is not known. The lobula plate contains cells that run tangentially to the retinal columns and sum the motion responses of the medulla across the visual field. The output of these Lobula Plate Tangential Cells (LPTCs) encode the wide-field motion of the visual scene. Interneurons mediate these signals to the motor neurons in the thoracic ganglia, enabling motor centers to move the head or body in response to the wide-field motion [5].

Such interneurons that communicate wide-field visual cues with the motor networks are critical because such cues are primarily generated by the animal's own motion. Therefore, minimizing the optic flow is one way that insects may stabilize their gaze or posture. Simulating wide-field motion by displaying moving patterns that envelop the animal have been used to evoke the "optomotor response", wherein the animal turns its neck [6], adjusts its posture [7], or walks along a curve [8] in an attempt to cancel out this visual motion. Implementing such a system on board a robot may enable us to enhance the postural stability of the robot, while providing an opportunity to model how animals may use optic flow information to direct walking. Some robots have also used optic flow to avoid barriers while walking [9]. As a proof of concept, we model the robot as a single neck actuator that can rotate the "head".

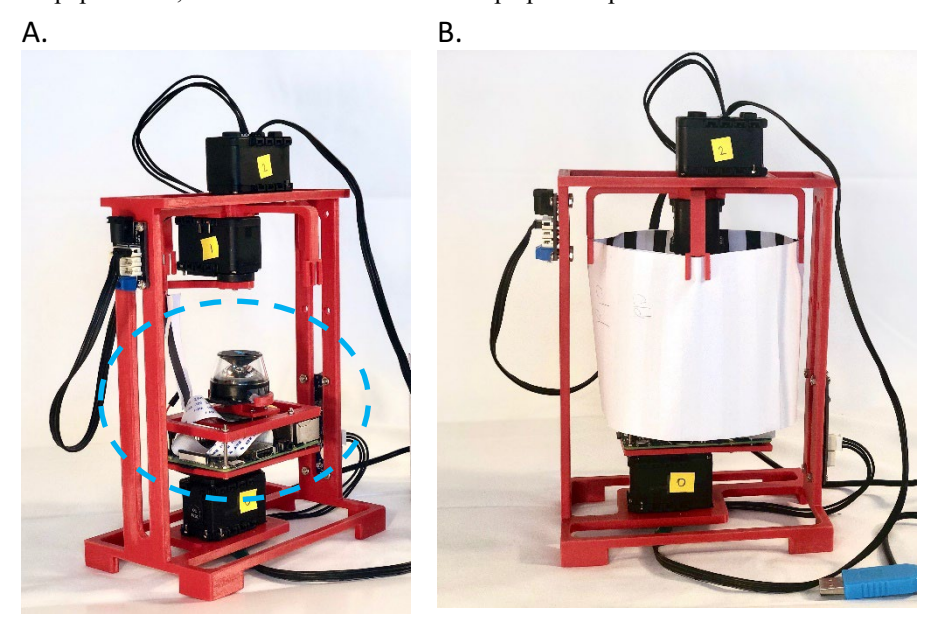
In this manuscript, we describe the robotic hardware and our neural modeling approach. We summarize the structure of the insect lobe and explain the simplifications and assumptions we made while constructing our model. We show that the layers within our model perform the computations observed or hypothesized to occur in the animal. We show that the result of the visual processing is a rate-coded estimate of the speed and direction of the background's motion. We show that by using the output of the model to stimulate motor neurons that actuate the neck, our robot acts as a closed-loop dynamical neuromechanical model of the insect optomotor response. Finally, we discuss how this system will be expanded in the future in order to incorporate more features present in the insect optic lobe, while increasing its utility for robotic vision.

## 2 Methods

#### 2.1 Robotic Hardware

Figure 1 presents the robotic hardware. The "head" consists of a Raspberry Pi with the Camera Module, equipped with a 360-degree lens (Figure 1A). The head is rotated by

one Dynamixel smart servo (Robotis, Seoul, South Korea). The "background" consists of a paper drum, the inside of which has a stripe pattern printed onto it. This is meant



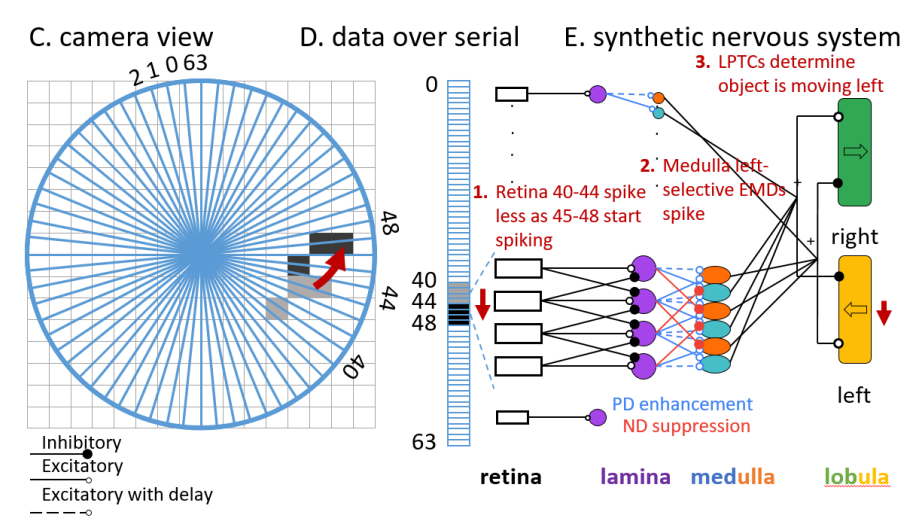


Figure 1 – Illustration of the robot hardware and SNS organization. A. The Raspberry Pi is equipped with the Camera Module. The blue dashed line encircles the Pi, camera, and 360-degree lens, which are assembled into a "head". B. The head rotates inside of a mobile background cylinder. C. The camera sees a radial image. The Pi sums the grayscale intensity of each bin and sends that value over a serial connection to the retina of the SNS. D. The retina transduces the intensity of the bins into the firing frequency of spiking neurons. E. The rest of the SNS performs lateral inhibition (lamina), generates direction-specific activity with EMDs (medulla), and then sums all EMD output to determine the motion of the background (LPTCs).

to mimic the experimental setup of studies of the insect optomotor response [8]. The head and background are connected to the same 3D printed chassis (Figure 1B).

The SNS model of the optic lobe runs on a laptop computer separate from the Raspberry Pi. The Pi processes and sends the data to the laptop over a serial connection by the following process. 64 x 64-pixel grayscale video is recorded and dissected for static images at about 25 Hz. Such low image resolution reduces serial traffic and is consistent with insects' comparatively low visual resolution [1]. This image is sorted into 64, 5.6 degree-wide angular "bins" along the azimuth, wherein each bin's intensity value is the average of all pixels it encapsulates (illustrated in Figure 1C). Note that this system only "sees" along one axis, the azimuth; it cannot detect changes in the elevation direction. When a bin's intensity value changes in subsequent images, it is flagged for transmission over serial to the SNS in the next data sentence (Figure 1D). Such a system reduces the length of sentences and thus increases the system's bandwidth.

Visual information from the camera is transduced into neural inputs at the retina layer of the optic lobe model (Figure 1E). Each angular bin in the camera's field of view has a corresponding retinal cell. The average grayscale intensity of each bin is mapped to an applied current for the retinal cell with black mapping to a current of 0 nA, white mapping to a current of 20 nA, and intermediate values mapping in a graded way. Each retinal cell represents the first layer of a columnar network that enhances contrast, detects changes in pixels, and sums these changes over the field of view to compute wide-field visual velocity. This network is described in detail in Section 2.3.

The connection between the robot and the SNS is bidirectional. The SNS possesses motor neurons (MNs) for the "neck" of the robot to rotate the camera around the vertical axis. There are two MNs, each of which rotates the neck in the opposite direction. In our previous work, we found that the motor output of small animals can be approximated by using the sum of the MN voltages to set the servo's speed and using the difference of the MN voltages to set the servo's equilibrium angle [10]. If the commanded angle or speed of the servo changes, then a new command sentence is sent over serial from the SNS controller to the robot.

#### 2.2 Synthetic Nervous System Organization and Design

The SNS model of the optic lobe is implemented with Animatlab [11] and its Robotics Toolkit [12]. Animatlab is an open-source 3D neuromechanical simulation software tool for simulating biologically-inspired organisms, robots, and neural networks. We wished to build a network that is biologically plausible but possible to run in real time. While the optic lobes of different insect species have behavior-specific visual processing networks, the overall structural organization is common for several kinds of arthropods including moths, flies, crabs, and mantises [13]. Since we are modeling a fundamental behavior observed in many species, we have combined information from multiple species. However, modeling more species-specific behaviors (e.g. mantis prey capture) would require modifying the network in species-specific ways.

**Neural Modeling Techniques.** Our network model is composed of integrate-and-fire neurons [14]. To simplify the description of the neurons, we write the equations in terms

of U, the membrane voltage above the neuron's rest potential [15]. In addition, each neuron has a membrane conductance  $G_m = 1$  and a constant spiking threshold  $\theta = 1$ . The resulting dynamics of a neuron can be written as

$$\tau_m \cdot \frac{dU}{dt} = -U + I_{app} + I_{tonic} + \sum_{i=1}^n G_{s,i} \cdot (\Delta E_{s,i} - U)$$
 (1)

if 
$$U \ge \theta$$
,  $U(t) \leftarrow 0$ , (2)

where  $\tau_m$  is the membrane time constant,  $I_{app}$  is an applied current,  $I_{tonic}$  is a constant intrinsic current, n is the number of incoming synapses,  $G_{s,i}$  is the instantaneous conductance of the  $i^{th}$  synapse (computed below), and  $\Delta E_{s,i}$  is the reversal potential of the  $i^{th}$  incoming synapse relative to the postsynaptic neuron's resting potential. Each synapse's instantaneous conductance is reset to its maximum value  $g_{s,i}$  when the presynaptic neuron spikes:

$$\tau_s \cdot \frac{dG}{dt} = -G \tag{3}$$

if presynaptic neuron spikes, 
$$G \leftarrow g$$
. (4)

In the following sections, we describe the desired function of connections within the network in terms of "gain" k, that is, the ratio between the postsynaptic and presynaptic neurons' spiking frequencies. Using our functional subnetwork approach for designing dynamical neural models, we can relate the gain to the neural and synaptic parameters, and directly tune their values [15].

#### 2.3 Structure and Function of the Optic Lobe Model

**Retina.** The retina layer encodes visual information into the neural system. The retina cells respond to changes in light intensity in the visual field. The compound eye of the retina has a hexagonally-arranged structure of ommatidia, i.e. photoreceptors that lie below the lens. Insects have multiple retina cells per ommatidium [16]. However, to keep the model tractable, our model simply possesses one retina cell per ommatidium.

The retina layer in our network consists of 64 neurons that each take input from the corresponding angular bins described in Section 2.1 (Figure 1E, white rectangles) Each neuron's applied current is a linear function of the average grayscale intensity of its corresponding optical bin. For simplicity, our retina only encodes *increases* in brightness, the so-called ON-ON pathways [3]. How this selection affects the performance of the motion detector is further explained in the medulla section. The retina neurons in our model have a time constant  $\tau_m = 200$  ms and a tonic current  $I_{tonic} = 0.5$  nA. These values ensure that the lamina neurons do not fire any spikes at the minimum input intensity and fire spikes at 100 Hz at the maximum input intensity.

**Lamina.** The lamina neurons function as a spatial filter, increasing the dynamic range of retina activity. Every neuron is excited by retina cells in its own column and inhibited by those from the adjacent columns, a connectivity pattern called lateral inhibition. This connectivity increases the contrast of the image.

In our model, the lamina layer consists of 64 neurons (Figure 1E, violet circles). Every neuron in the lamina is excited by a corresponding neuron in the retina, and inhibited by the retina neurons of the neighboring columns (Figure 1E). The lamina neurons have the same parameter values as the retina neurons. To cancel the lamina's response to a spatially uniform image, we wish for the gain of the incoming synapses to add to 0. Since each lamina cell receives excitation from one retina cell but inhibition from two, we designed the excitatory synapses to have a gain of 1.5 and the inhibitory synapses to have a gain of -0.25. For the excitatory synapses,  $\Delta E_s = 160$  mV and  $g_s = 1.064 \,\mu\text{S}$ ; for the inhibitory synapses,  $\Delta E_s = -80$  mV and  $g_s = 0.3072 \,\mu\text{S}$ . Both synapse types have time constants  $\tau_s = 2.17$  ms.

Medulla. The cells in the medulla respond to visual motion in a direction-dependent manner. The classical Reichardt detector structure computes the correlation of one column's activity with a time-delayed copy of a neighboring column's activity. This two-column comparison excites the medulla neuron in the "preferred direction". This model successfully predicts many gross features of motion vision in insects [3]. Recent neurophysiology suggests a new, "three-arm detector" model that combines preferred direction enhancement (the Reichardt detector) and null direction suppression (the Barlow-Lewick detector) [17]. Combining these mechanisms not only accurately replicates the response properties of the T4 and T5 cells in the medulla, but also accounts for the non-negative nature of signal transmission throughout the nervous system (i.e. neurons only spike when depolarized, not when hyperpolarized).

Our medulla model is based on the "three-arm detector" model [3]. Each layer possesses 126 neurons, half of which are excited by rightward visual motion, and half of which are excited by leftward motion. These correspond to the medulla's T4 neurons [3]. Figure 1E shows the medulla neurons (blue and orange circles), each of which receives an excitatory input from its corresponding lamina neuron, a delayed excitatory signal from its neighboring column's lamina neuron, and a delayed inhibitory signal from the contralateral lamina neuron. To perform the multiplication inherent to the Reichardt model, each medulla neuron operates as a logical AND gate. Specifically, it can only fire action potentials if is depolarized by both excitatory inputs simultaneously. The duration of its spiking encodes the speed of visual motion across those two columns of the optic lobe. To enforce AND gate functionality and prevent the medulla neurons from firing when only one excitatory input is present, each neuron's tonic stimulus  $I_{tonic} = -19.5$  nA. Otherwise, all parameter values are the same as the other neurons. All excitatory synapses have k = 1 and all inhibitory synapses have k = -1. For the excitatory synapse,  $\Delta E_s = 160$  and  $g_s = 0.658 \,\mu\text{S}$ . The neighboring column's excitatory synapse additionally has a delay  $\Delta t = 100$  ms. For the inhibitory synapse,  $\Delta E_s = -80 \text{ mV}$  and  $g_s = 1.536 \mu\text{S}$ .

**Lobula Plate Tangential Cells.** The lobula plate tangential cells (LPTCs) are large, motion-sensitive neurons that reside in the posterior lobula plate. They can be separated into four different layers, each activated by large-field motion in one of the four cardinal motion directions. They pool the output signals on their dendrites from many thousands of directionally-selective neurons [3]. The LPTCs depolarize in response to background

motion in their preferred direction and hyperpolarize in response to motion in their null direction. The LPTCs, however, do not compute motion locally but rather integrate over a large part of the visual field. The lobula plate tangential cells inhibit each other such that right inhibits left and vice versa, and up inhibits down and vice versa [3]. These cells are commonly thought to detect optical flow that arises from self-motion.

In our model, the LPTCs sum the outputs of the T4 cells in the medulla in a directionally-selective way. We only model the right- and left-sensitive LPTCs. Figure 1E shows how the medulla neurons all feed into one of two LPTCs. These neurons have the same properties as the rest of the network. The synapses from the medulla to the LPTCs have the same properties as those from the lamina to the medulla. None of these synapses possess delays.

**Motor Neurons.** The motor centers receive input from the LPTCs via descending interneurons [5]. We modeled such connections by synapsing the LPTC neurons onto nonspiking neurons that represent the combined motor neuron (MN) and muscle membrane. These MNs function as leaky integrators, integrating incoming spikes over time but "leaking" to 0 activity when no spikes are incoming. These neurons have the same parameter values as the other neurons in the network, except that the spiking mechanism has been disabled. As described above, the MN voltages specify rotation and speed commands for the neck servomotor.

## 3 Results

**LPTC voltage encodes wide-field visual motion.** Figure 2 displays raster plots of retina, lamina, and medulla spiking activity in response to background motion. Each point represents one action potential. The retina encodes the stripe pattern of the background as it moves right for five seconds, and then left for five seconds. The lamina increases the contrast by amplifying range of firing frequencies seen in the retina (Figure 3). The medulla neurons encode the direction of the background's velocity, with separate subpopulations encoding each direction. Each one of these layers encodes visual information as observed in animal systems.

**LPTC** activity reflects wide-field pattern velocity. Figure 4 shows how the LPTC neurons encode the velocity of the background. The LPTC spikes have been removed from the membrane voltage curves to more clearly show how the LPTC depolarization (solid lines) encodes the velocity of the background (dotted lines). However, when the background's speed becomes too high, the correlation operation performed by the medulla breaks down, and the LPTC voltage no longer reflects the background speed. This same phenomenon is observed in *Drosophila* [3].

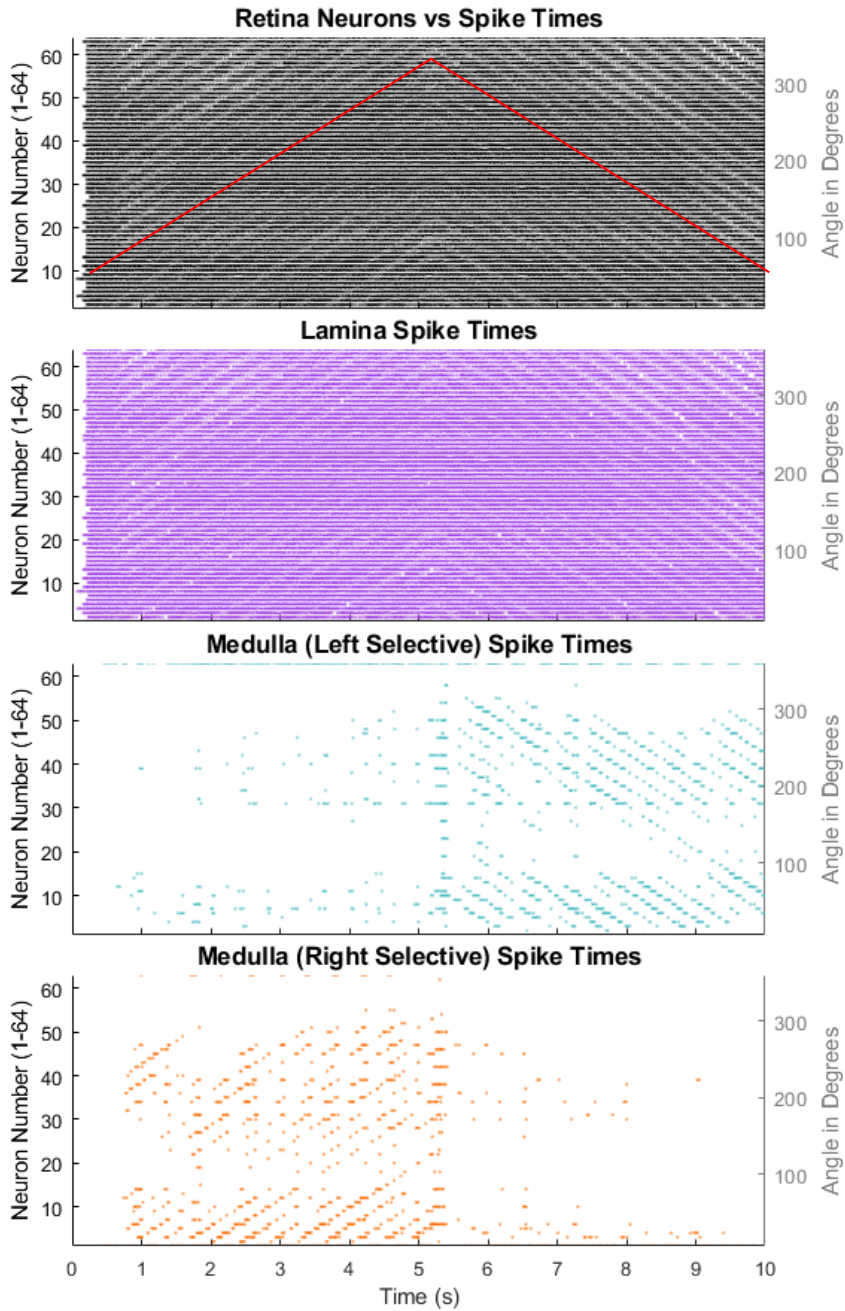


Figure 2 – Raster plots showing the spike times of each neuron (left axis) in each layer in response to background motion. The red line indicates the angle of the background (right axis). The retina encodes the motion, the lamina activity follows that of the retina, the left-selective medulla cells are active during leftward pattern motion, and the right-selective medulla cells are active during rightward motion. Colors match the anatomy in Figure 1.

#### The robot successfully tracks a background pattern via the optomotor response.

Figure 5 shows that the complete, closed-loop system can generate a functional optomotor response even as the movement of the background increases in frequency. The velocity of the neck tracks that of the background, even though the absolute orientation of the head and background are different. This is because the visual system has no specific landmarks to track. Because the system is closed-loop, neck rotation impacts the observed velocity of the background.

## 4 Discussion

In this manuscript, we built a synthetic nervous system (SNS) model of parts of the insect optic lobe, and used it to model the optomotor response observed in insects [3, 6–8]. We applied the functional subnetwork approach [15] to tune the known and hypothesized anatomical structure of the insect optic lobe without any machine learning or optimization. The resulting network can process video data in real time (albeit more slowly and at lower resolution than its biological counterparts), enhance its contrast, compute its motion, and control the motion of a "head" as it attempts to stabilize its gaze on the background. Such a system serves as a robotic model of visual processing in insects, which can be used to consolidate results from different experiments and species into one self-consistent model. Additionally, this system will form the basis of more sophisticated visually-guided robotic behaviors in the future.

Despite the detail of our model, some known features of insect visual systems are not yet incorporated. To reduce the complexity of the model, we modeled one-dimensional (azimuthal, or left-right) vision only. Insects possess dedicated processing pathways to see along the vertical axis as well [3], and thus our future work will expand the structure of this network into an additional dimension. To further reduce the complexity of the model, we only modeled ON pathways, that is, pathways that respond to transitions from darkness to light, and omitted OFF pathways. However, both are known to

## Lateral Inhibition Increases the Lamina's Dynamic Range Relative to the Retina's

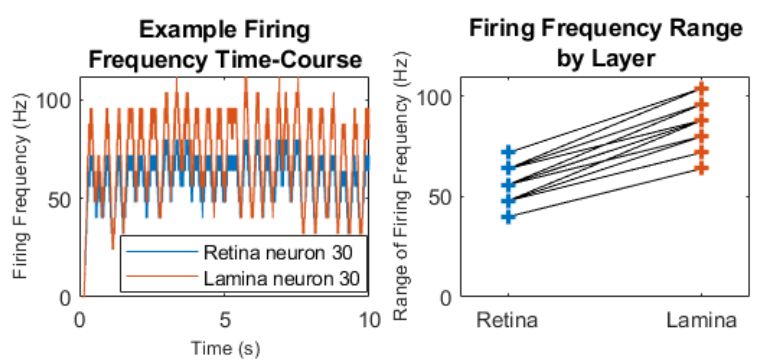


Figure 3 – (Left) The range of firing frequencies in the lamina appear to be higher than those in the retina. (Right) Comparing each lamina neuron's range of firing frequencies to that of its corresponding retina neuron confirm this.

play a role in the processing of motion vision [3]. In our future work, we will explore the impact of incorporating these additional (but seemingly redundant) pathways.

Our ultimate goal is to implement this model of insect vision onboard our insect-like

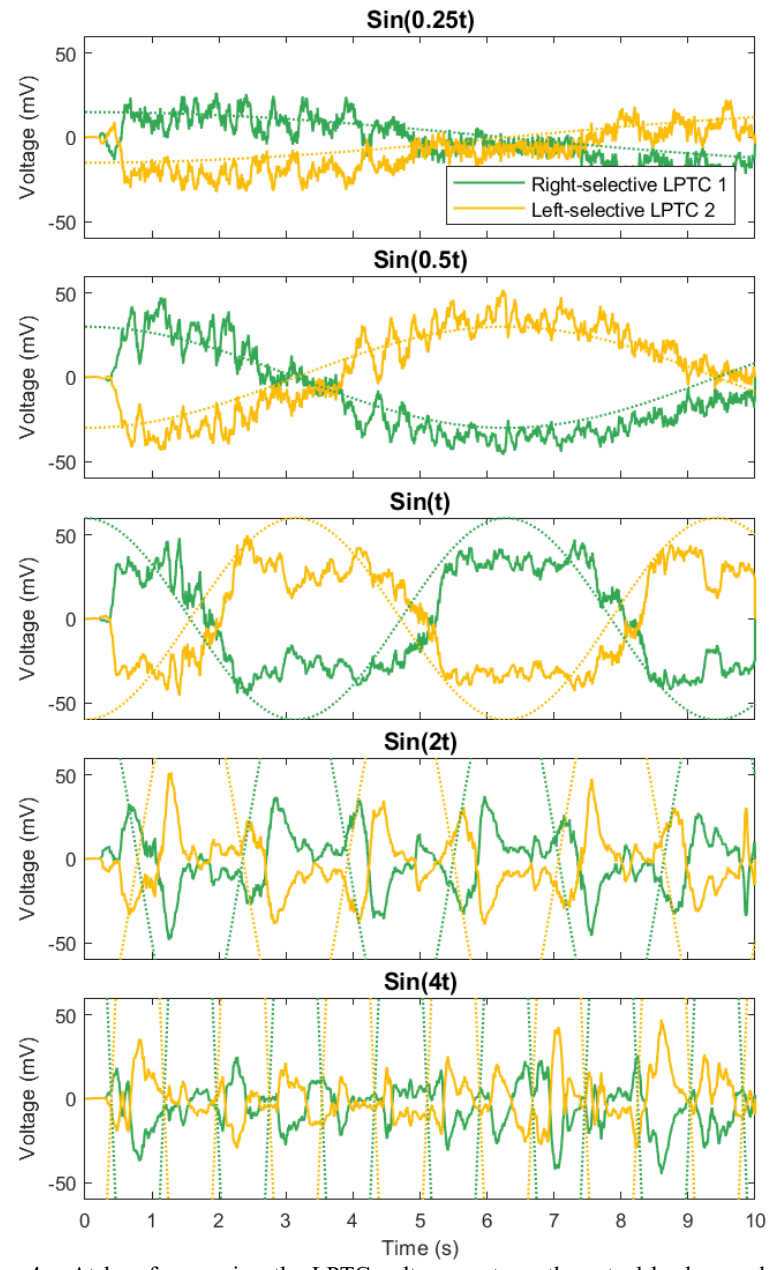


Figure 4 – At low frequencies, the LPTC voltage captures the actual background velocity (dotted lines). However, at high frequencies, the LPTC response amplitude decreases and its phase lags behind the actual velocity, meaning it cannot encode such rapid motions.

hexapod robot, MantisBot [12]. In our past work, we have studied how descending commands from the brain may alter leg-local reflexes to direct walking behaviors [18]. We anticipate that descending pathways that mediate the optomotor response observed in walking insects will provide additional information with which MantisBot can stabilize its posture. We also anticipate that the gaze stabilization afforded by the optomotor response will make MantisBot more capable of identifying prey-like visual stimuli moving against the background. Such a system will enable us to generate and test hypothetical sensorimotor control networks both to consolidate results from neuroethology into one cohesive model, and to propose novel control algorithms for legged robots.

#### References

- Egelhaaf, M., Boeddeker, N., Kern, R., Kurtz, R., Lindemann, J.P.: Spatial vision in insects is facilitated by shaping the dynamics of visual input through behavioural action. Front. Neural Circuits. 6, 1–23 (2012).
- Bagheri, Z.M., Wiederman, S.D., Cazzolato, B.S., Grainger, S., O'Carroll, D.C.: Performance of an insect-inspired target tracker in natural conditions. Bioinspir. Biomim. (2017).
- Borst, A., Haag, J., Mauss, A.S.: How fly neurons compute the direction of visual motion. J. Comp. Physiol. A Neuroethol. Sensory, Neural, Behav. Physiol. (2019).
- 4. Webb, B.: Robots with insect brains. Science (80-.). 368, 244–245 (2020).
- 5. Suver, M.P., Huda, A., Iwasaki, N., Safarik, S., Dickinson, M.H.: An Array of Descending Visual Interneurons Encoding Self-Motion in Drosophila. J. Neurosci. (2016).
- Rossel, S.: Foveal fixation and tracking in the praying mantis. J. Comp. Physiol. A. 139, 307–331 (1980).
- Nityananda, V., Tarawneh, G., Errington, S., Serrano-Pedraza, I., Read, J.: The optomotor response of the praying mantis is driven predominantly by the central visual field. J. Comp. Physiol. A Neuroethol. Sensory, Neural, Behav. Physiol. 203, 77–87 (2017).
- 8. Dürr, V., Ebeling, W.: The behavioural transition from straight to curve walking: kinetics of leg movement parameters and the initiation of turning. J. Exp. Biol. (2005).
- Meyer, H.G., Klimeck, D., Paskarbeit, J., Rückert, U., Egelhaaf, M., Porrmann, M., Schneider, A.: Resource-efficient bio-inspired visual processing on the hexapod walking robot HECTOR. PLoS One. 15, e0230620 (2020).
- Szczecinski, N.S., Goldsmith, C.A., Young, F.R., Quinn, R.D.: Tuning a Robot Servomotor to Exhibit Muscle-Like Dynamics. Conference on Biomimetic and Biohybrid Systems. (2019).
- 11. Cofer, D.W., Cymbalyuk, G., Reid, J., Zhu, Y., Heitler, W.J., Edwards, D.H.: AnimatLab: a 3D graphics environment for neuromechanical simulations. J. Neurosci. Methods. (2010).
- Szczecinski, N.S., Chrzanowski, D.M., Cofer, D.W., Terrasi, A.S., Moore, D.R., Martin, J.P., Ritzmann, R.E., Quinn, R.D.: Introducing MantisBot: Hexapod robot controlled by a high-fidelity, real-time neural simulation. In: IEEE International Conference on Intelligent Robots and Systems. pp. 3875–3881. Hamburg, DE (2015).
- Joly, J.-S., Recher, G., Brombin, A., Ngo, K., Hartenstein, V.: A Conserved Developmental Mechanism Builds Complex Visual Systems in Insects and Vertebrates. Curr. Biol. (2016).
- Mihalas, S., Niebur, E.: A generalized linear integrate-and-fire neural model produces diverse spiking behaviors. Neural Comput. 21, 704

  –718 (2009).
- 15. Szczecinski, N.S., Hunt, A.J., Quinn, R.D.: A functional subnetwork approach to designing synthetic nervous systems that control legged robot locomotion. Front. Neurorobot. 11,

(2017).

- 16. Borst, A.: Neural Circuits for Elementary Motion Detection. J. Neurogenet. (2014).
- 17. Barlow, H.B., Levick, W.R.: The mechanism of directionally selective units in rabbit's retina. J. Physiol. 477–504 (1965).
- Szczecinski, N.S., Getsy, A.P., Martin, J.P., Ritzmann, R.E., Quinn, R.D.: MantisBot is a Robotic Model of Visually Guided Motion in the Praying Mantis. Arth. Struct. Dev. (2017).

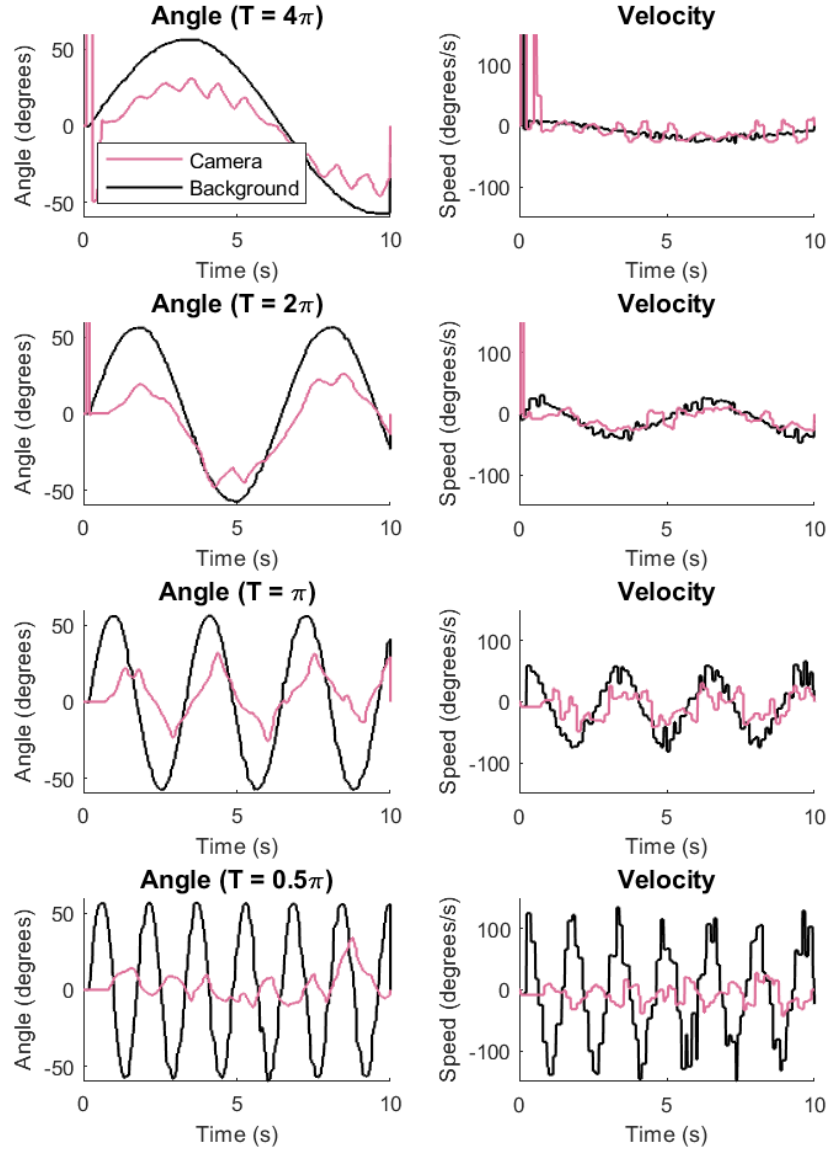


Figure 5 – The robot's optomotor response enables it to track wide-field visual motion. At low speeds (top), the camera's angle and velocity follow those of the background. However, when the background moves too rapidly (bottom), the response degrades, as expected.